ELSEVIER

Journal of Alloys and Compounds 320 (2001) 199–206

Journal of ALLOYS AND COMPOUNDS

www.elsevier.com/locate/jallcom

Some experiences modelling the sigma phase in the Ni–V system

A. Watson[a,*], F.H. Hayes[b]

[a]School of Process, Environmental and Materials Engineering, The University of Leeds, Leeds LS2 9JT, UK
[b]Materials Science Centre, University of Manchester, Institute of Science and Technology, Grosvenor St., Manchester M1 7HS, UK

Abstract

A number of thermodynamic optimisations of the Ni–V system have been carried out using experimental phase diagram and thermodynamic data available from the literature. In each optimisation, a different model was used to describe the thermodynamic properties of the sigma phase. The results of the optimisations have been compared with each other and their shortcomings discussed.

Keywords: Thermodynamic optimisation; Ni–V system; Modelling; Sigma phase

1. Introduction

Of fundamental importance to alloy design and development is a thorough knowledge of phase equilibria with respect to temperature, composition and, if appropriate, pressure of the alloy system under study. In order to be confident that a component will perform to specification during its service life, it is necessary to know that the chemistry of the material will not change in such a way as to lead to premature failure.

Thermodynamic modelling of phase equilibria is becoming an increasingly important tool in the design of new materials. With appropriate thermodynamic models and databases, it is possible to explore the phase constitution of multicomponent systems with only a minimal amount of experimental effort to test the results of the calculations. Indeed, in some cases, it is possible to predict the formation of certain phases which may only physically appear after prolonged exposure to high temperature, for example, as the material slowly approaches equilibrium. A good example is the case of sigma phase precipitation in Ni-based superalloys. The sigma phase is a hard brittle intermetallic phase, which may well not be present in a structure during the fabrication of a particular component. However, at high service temperatures, the phase may precipitate as chemical equilibrium is approached, accompanied by a deleterious effect on mechanical properties. It is important, therefore, to have good thermodynamic descriptions which can be extrapolated to higher order systems with confidence.

The sigma phase appears in 53 binary systems [1] containing one element from group V_A or VI_A of the Periodic Table (type-A element) and one element from the first, second or third long period (type-B). Some of these have been modelled successfully [2]. Interestingly, although the sigma phase appears in a number of ternary systems containing nickel (Ni–Cr–W, Ni–Cr–Si, Ni–Cr–Fe, Ni–V–Co), it is stable in only one nickel-containing binary system, Ni–V.

In this work are reported the results of modelling the Ni–V system using a number of different models for the sigma phase.

2. The Ni–V system

It is not the intended purpose of this article to present a complete assessment of the system; this will be published elsewhere. However, as the optimisation process involves the use of experimental information it is necessary to give some indication of the data available.

Assessments of the system are available in the literature [3–5] but only the latest gives optimised thermodynamic parameters.

The phase diagram is well described across the whole composition range by a number of key publications [6–10]. It is characterised by a large fcc phase field which extends almost half-way across the diagram. There is also an appreciable dissolution of Ni in V(bcc), up to a maximum of 24 at% Ni at 1280°C [8]. In between the fcc

*Corresponding author. Tel.: +44-113-233-2354.
E-mail address: a.watson@leeds.ac.uk (A. Watson).

0925-8388/01/$ – see front matter
PII: S0925-8388(00)01472-9

and bcc phases there is a large σ-phase field spanning about 20 at% at low temperatures. In common with systems such as Co–V [11], the σ-phase is in equilibrium with the liquid phase at higher temperatures. It has also been suggested that a transition exists in this phase between high and low temperature forms [6,8,12], although this feature has not been modelled in this work.

Three other intermetallic phases are present in the system, Ni_3V, Ni_2V and NiV_3, the first showing a reasonable homogeneity range at ~4 at% at 900°C. A fifth intermetallic phase may also exist, Ni_8V [13].

Heats of mixing of the liquid phase [14] and of formation of the solid solution phases [15] have been measured by calorimetry. $\overline{G}_V$ and $\overline{G}_{Ni}$ in the fcc-phase have been measured by emf and a combination of diffusion couple and vaporisation techniques [16–19]. Thermodynamic data also exist for the intermetallic compounds (ΔH_f (Ni_3V) [20,21], $\Delta H_{Tr}(Ni_3V \rightarrow fcc)$ and $\Delta H_{Tr}(Ni_2V \rightarrow fcc)$ [22], $\Delta H_{decomp}(NiV_3 \rightarrow bcc + \sigma)$ [8]).

3. Optimisation procedure

Four different optimisations were performed, the main difference between them being the model chosen to represent the Gibbs energy of the σ-phase in each case. The procedure adopted was essentially the same in each optimisation. Models were chosen to represent the Gibbs energy of each phase, where possible appropriate to its crystal structure. Temperature and composition dependent parameters of the Gibbs energy expressions were adjusted during the optimisation using a least-squares fitting computer program so that the differences between the experimental data and corresponding values generated from the optimised Gibbs energy expressions were minimised. In this way, a set of Gibbs energy expressions were produced which is consistent with the phase diagram and thermodynamic properties of the system.

3.1. Thermodynamic descriptions of the pure elements

Data for the pure elements were taken from the compilation of Ref. [23]. The reference states chosen were the stable states at 298.15 K (SER).

3.2. Models for the liquid, fcc and bcc phases

These three phases were described using the same substitutional solution model in each optimisation. The Gibbs energy of each of the phases is expressed as

$$G^{\phi} = x_{Ni}\,{}^{0}G^{\phi}_{Ni} + x_V\,{}^{0}G^{\phi}_{V} + RT(x_{Ni}\ln x_{Ni} + x_V \ln x_V) + G^{E} \quad (1)$$

where ${}^{0}G^{\phi}_{Ni}$ and ${}^{0}G^{\phi}_{V}$ are the unary descriptions of pure Ni and pure V with the structure ϕ (liquid, fcc or bcc). G^E is the excess Gibbs energy. The excess Gibbs energy is described by the Redlich–Kister polynomial [24]:

$$G^{E} = x_{Ni}x_V\sum_{i=0}^{n} {}^{i}L(x_{Ni} - x_V)^i \quad (2)$$

where ${}^{i}L$ are adjustable parameters and take the form $a + bT$.

3.3. Ni_2V and NiV_3

These compounds were treated as stoichiometric phases.

3.4. Ni_3V

This phase was treated as a stoichiometric phase in the first optimisation. However, in subsequent optimisations, the stoichiometry range of the phase was treated using the Wagner–Schottky model [25]. This can be expressed in the form of the compound energy model, where two sublattices are assumed for the phase, with Ni atoms occupying the sites in sublattice 1 and V atoms the sites in sublattice 2 for ideal stoichiometry. In order to model the stoichiometry range, V atoms occupy Ni sites and Ni atoms occupy V sites as antisite defects. The Gibbs energy of the phase is given as [26]

$$\begin{aligned} G(Ni_3V) = {} & 4(x_{Ni}\,{}^{0}G^{fcc}_{Ni} + x_V\,{}^{0}G^{bcc}_{V} \\ & + RT[3(y'_{Ni}\ln y'_{Ni} + y'_V \ln y'_V) + (y''_{Ni}\ln y''_{Ni} \\ & + y''_V \ln y''_V)] + \Delta G_{Ni:V}\cdot y'_{Ni}\cdot y''_V + \Delta G_{Ni:Ni} \\ & \cdot y'_{Ni}\cdot y''_{Ni} + \Delta G_{V:V}\cdot y'_V\cdot y''_V + \Delta G_{V:Ni}\cdot y'_V\cdot y''_{Ni} \\ & + \sum_{i=0}^{n}[{}^{i}L_{Ni,V:V}\cdot y'_{Ni}\cdot y'_V\cdot(y'_{Ni} - y'_V)^i\cdot y''_V \\ & + {}^{i}L_{Ni,V:Ni}\cdot y'_{Ni}\cdot y'_V\cdot(y'_{Ni} - y'_V)^i\cdot y''_{Ni} \\ & + {}^{i}L_{Ni:V,Ni}\cdot y'_{Ni}\cdot y''_V\cdot y''_{Ni}(y''_{Ni} - y''_V)^i + {}^{i}L_{V:V,Ni} \\ & \cdot y'_V\cdot y''_V\cdot y''_{Ni}(y''_{Ni} - y''_V)^i] \end{aligned} \quad (3)$$

The ΔG terms represent the 'compound' Gibbs energies and the ${}^{i}L$ terms the excess Gibbs energies of mixing of the species on each sublattice. The Gibbs energy of the phase is given relative to fcc-Ni and bcc-V.

3.5. The σ-phase

Four different models were used for this phase, one in each of the optimisations.

3.5.1. Substitutional model

Firstly, a simple substitutional model, as used for the liquid, fcc and bcc phases, was employed. The BINGSS [27] optimisation software was used. A number of different combinations of parameters were used, but the best fit of the calculated to the experimental data was given with two parameters (two coefficients for each parameter) for

Table 1
Optimised parameters with the σ-phase treated as a substitutional solution

Phase	Parameter	Value
Liquid	${}^0L$	$-60\,577.89 + 14.71723T$
	${}^1L$	$-13\,534.30$
fcc	${}^0L$	$-65\,194.06 + 12.81340T$
	${}^1L$	$-21\,391.88$
Ni_3V	$\Delta_f G(Ni_{0.75}V_{0.25})$	$-15\,543.68 + 1.30975T$
Ni_2V	$\Delta_f G(Ni_{0.666}V_{0.333})$	$-22\,880.43 + 7.103T$
sigma	${}^0L$	$-78\,921.00 + 6.93777T$
	${}^1L$	$-15\,994.01$
bcc	${}^0L$	$-48\,802.78 + 15.10139$
	${}^1L$	$-19\,042.26$
NiV_3	$\Delta_f G(Ni_{0.25}V_{0.75})$	$-14\,940.48 + 6.30919$

each phase. The optimised data are given in Table 1, and the calculated phase boundaries together with the experimental data are given in Fig. 1. The diagram was calculated using the Binaire calculation program [28]. However, the overall fit is quite poor.

3.5.2. CEF, three sublattices, $(Ni,V)_{18}(V)_4(Ni)_8$

Subsequent treatments used variations of the compound energy formalism (CEF) with different sublattice occupation. The reason for choosing this type of model is that it reflects the crystallography of the phase more closely than a simple substitutional model.

The Gibbs energy of a phase ϕ comprising three sublattices and an arbitrary number of components can be written as

$$G_m(\phi) = \sum_i \sum_j \sum_k y_i^1 y_j^2 y_k^3 \, {}^0G_{i:j:k} + RT \sum_s a_s \sum_i y_i^s \ln(y_i^s) + {}^E G \tag{4}$$

where y_i^s represents the site fraction of component i on each sublattice s, and the ${}^0G_{i:j:k}$ terms represent the 'compound energies' or 'end-members' which are essentially the Gibbs energies of formation of the phase when each sublattice is completely occupied by only one constituent. The term a_s is the relative number of sites on each sublattice.

Mixing on each sublattice is assumed to be random, and the excess Gibbs energy associated with mixing, ${}^E G$, is given as

$$\begin{aligned} {}^E G_m(\phi) = & \sum_{i_1} \sum_{i_2} \sum_j \sum_k y_{i_1}^r y_{i_2}^r y_j^s y_k^t L_{i_1,i_2:j:k} + \cdots \\ & + \sum_{i_1} \sum_{i_2} \sum_{j_1} \sum_{j_2} \sum_k y_{i_1}^r y_{i_2}^r y_{j_1}^s y_{j_2}^s y_k^t L_{i_1,i_2:j_1,j_2:k} + \cdots \end{aligned} \tag{5}$$

The first L parameter given above (for a binary system) is the excess Gibbs energy mixing parameter for the mixing of two elements on one sublattice. The second L parameter relates to the case when mixing occurs on two sublattices. Each L parameter is described as a function of temperature and composition as in the case of a substitutional solution.

The unit cell of the σ-phase contains 30 atoms which lie on five crystallographically independent sublattices. In the unit cell, the occupancy of the five sublattices is two, four, eight, eight and eight atoms, with coordination numbers 12, 15, 14, 12 and 14, respectively, and neutron diffraction studies have given an indication of the preferential occupancy of each sublattice by each element [29]. Ideally, the phase should be modelled using the CEF with five sublattices. However, this would result in the need for 32 end-member parameters, which is far too many to produce a meaningful modelling of the phase.

Early attempts at modelling the σ-phase using the CEF considered only three sublattices with mixing on just one. A stoichiometry of $(A,B)_{18}(A)_4(B)_8$ was used successfully for the modelling of the σ-phase in the Fe–Cr [30] and Fe–V [31] systems, the Fe atoms represented by B in each case. This reduced substantially the number of optimising parameters. In order for the modelling of the Ni–V σ-phase to be compatible with these assessments the same model was chosen here in the second optimisation — $(Ni,V)_{18}(V)_4(Ni)_8$. This model has also been used for the Ni–V σ-phase in [5].

The optimised parameters are given in Table 2 and the phase diagram, calculated using MTDATA [32], is given in Fig. 2 along with the experimental data. The fit of the calculated phase boundaries to the experimental data is very good. However, this stoichiometry does create prob-

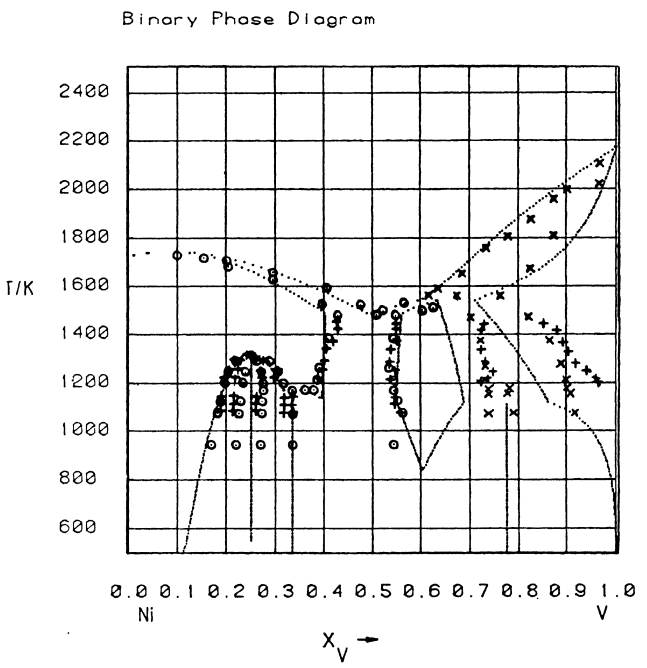

Fig. 1. The optimised Ni–V phase diagram, produced using a substitutional model for the σ-phase with two adjustable excess Gibbs energy parameters (Table 1).

Table 2
Optimised parameters with the σ-phase treated using the CEF, $(Ni,V)_{18}(V)_4(Ni)_8$

Phase	Parameter	Value
Liquid	${}^0L$	$-71\,012.38+26.85583T$
	${}^1L$	$-3070.39-0.71481T$
	${}^2L$	$19\,867.95-14.62151T$
fcc	${}^0L$	$-52\,549.13+14.49558T$
	${}^1L$	$-22\,796.85+9.02933T$
	${}^2L$	-6311.71
Ni_3V	$\Delta_f G_{Ni:V}$	$-51\,569.39+5.62961T$
	$\Delta_f G_{Ni:Ni}$	$4363.13-1.06473T$
	$\Delta_f G_{V:V}$	$32\,000.00+6.8T$
	$\Delta_f G_{V:Ni}$	$51\,569.39-5.62961T$
	${}^0L_{Ni,V:*}$	-6520.17
	${}^1L_{*:V,Ni}$	414.67
Ni_2V	$\Delta_f G(Ni_{0.666}V_{0.333})$	$-14\,680.94+2.15972T$
sigma	$\Delta_f G_{Ni:V:Ni}$	$5237.58-1.74417T$
$(Ni,V)_{18}(V)_4(Ni)_8$	$\Delta_f G_{V:V:Ni}$	$-11\,926.07+2.50991T$
	${}^0L$	$-34\,962.78+14.71808T$
	${}^1L$	$-96\,606.02+9.02933T$
bcc	${}^0L$	$-35\,446.36+14.67865T$
	${}^1L$	$349.61-2.94069T$
NiV_3	$\Delta_f G(Ni_{0.25}V_{0.75})$	$-10\,341.31+2.10677T$

lems in relation to the Ni–V system. The σ-phase field is quite wide, and experimental determinations suggest that it reaches a V content of 73.5 at% at the NiV_3 peritectoid temperature of 900°C [8]. This is at the very limits of the concentration range allowed by this model (73.3 at%), and would certainly not allow the extension of the σ-phase field to higher V contents upon the addition of a third element such as Si, a feature which has been suggested by Hall and Algie [1]. The consequences of the stoichiometry limit can be seen in the optimised Gibbs energy curve for the σ-phase. As can be seen in Fig. 3, the curve has an unusual, almost 'L' shape, and at lower temperatures the stability range is limited by the stoichiometry allowed by the model and not by the energetics of the phase itself in relation to the bcc-phase.

This stoichiometry problem is not uncommon and has led to implementation of new stoichiometries for the σ-phase model in order to give a wider possible composition range for the σ-phase field.

3.5.3. CEF, three sublattices, $(Ni,V)_{10}(V)_4(Ni,V)_{16}$

By combining sublattices with similar coordination numbers a stoichiometry of $(A,B)_{10}(B)_4(A,B)_{16}$ is achieved [2] and has been used successfully in an assessment of the Al–Nb system [33]. This model was used in the third optimisation with $(Ni,V)_{10}(V)_4(Ni,V)_{16}$ as the stoichiometry of the σ-phase. By introducing mixing on a second sublattice, however, the number of end-members is increased, resulting in an increase in the number of variable parameters in the optimisation. This makes it more difficult for the optimisation calculation to converge. Some simplifications can be made, however, as with this model the description allows for parameters corresponding to a lattice stability for pure V(σ). In this optimisation, the

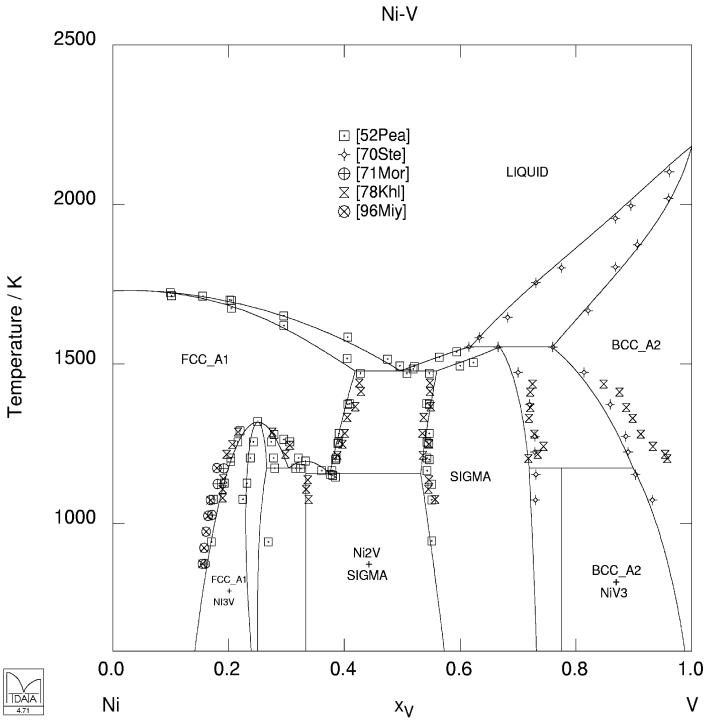

Fig. 2. The Ni–V phase diagram, calculated using the CEF model with a stoichiometry of 18:4:8 for the sigma phase.

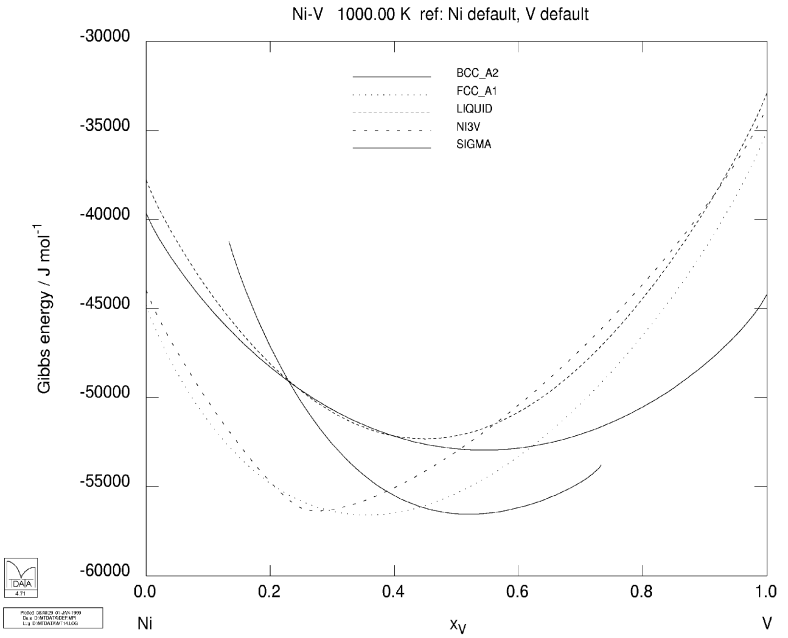

Fig. 3. Gibbs energy curves at 1000 K for phases in the Ni–V system, with the sigma phase calculated using the CEF with 18:4:8 stoichiometry. Referred to HSER. Gibbs energies of the stoichiometric phases have been omitted for clarity.

value for $G^{(\mathrm{bcc}\rightarrow\sigma)}$ was taken from the work of Hayes and Kubitz [34] and was fixed in the calculation. Figs. 4 and 5 show the phase diagram and the optimised Gibbs energy curves, calculated using Thermo-Calc [35] and the parameters in Table 3. It can be clearly seen that the Gibbs energy curve for the σ-phase stretches over a wider range of composition as expected from the stoichiometry of the model, and this easily covers the range observed experimentally. However, the fit of the optimised phase diagram to the experimental data is no better than experienced using the earlier stoichiometry. The thermodynamic description for this phase (Table 3) comprises very high values for the excess (L) parameters for the interactions of the Ni and V on the first and third sublattices. Mathematically, these high values are required in order to give the relatively smooth shape of the Gibbs energy curve required to fit the phase diagram data and, in fact, as can be seen by the fit to the experimental data points, this is still not sufficient to accurately model the system.

A strange kink appears in the Gibbs energy curve for the

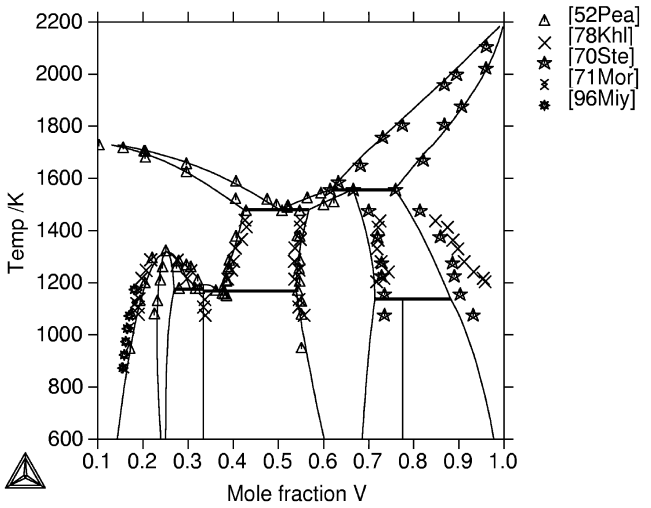

Fig. 4. The Ni–V phase diagram, calculated using the CEF model with a stoichiometry of 10:4:16 for the sigma phase.

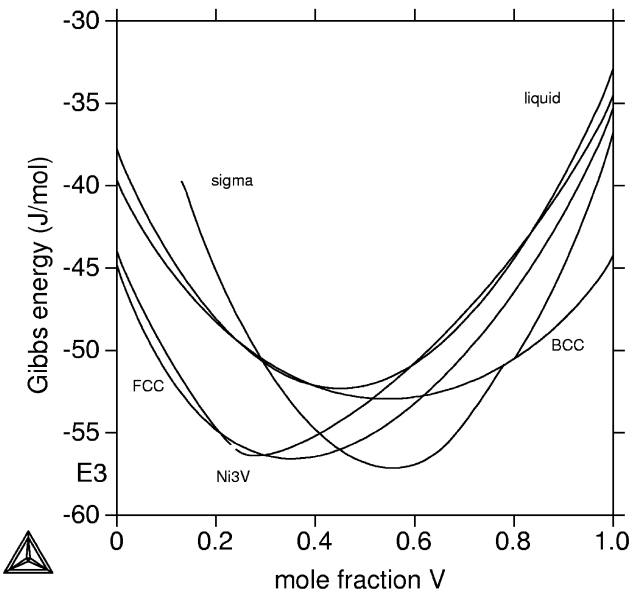

Fig. 5. Gibbs energy curves at 1000 K for phases in the Ni–V system, with the sigma phase calculated using the CEF with 10:4:16 stoichiometry, referred to HSER. The Gibbs energies of the stoichiometric phases have been omitted for clarity.

Table 3
Optimised parameters for the σ-phase using the CEF with the $(Ni,V)_{10}V_4(Ni,V)_{16}$ stoichiometry. Parameters for the other phases in the system are as given in Table 2

Phase	Parameter	Value
sigma	$\Delta_f G_{(Ni:V:Ni)}$	15 000
$(Ni,V)_{10}V_4(Ni,V)_{16}$	$\Delta_f G_{(Ni:V:V)}$	643 467.27 + 315.26082*T*
	$\Delta_f G_{(V:V:Ni)}$	679 100.78 + 362.7192*T*
	$\Delta_f G_{(V:V:V)}$	2 000 100 + 23.1*T*
	${}^0L_{(Ni,V:V:*)}$	34 550.83 + 59.13219*T*
	${}^0L_{(*:V:Ni,V)}$	359 345.45 − 140.786*T*

σ-phase, suggesting that the phase is not described very well by this optimised dataset.

3.5.4. The modified CEF model

The importance of configurational, configuration independent and excitational contributions to the Gibbs energy of mixing has been recognised for many years [36–39]. Unfortunately, the original CEF [40,41], widely adopted by the Calphad community, is a wholly configurational model (the excitational contributions are incorporated in the compound energies) in that every term in the Gibbs energy expression is a function of the sublattice fractions (y^s). The important but ignored configuration independent contributions, on the other hand, are a function of the mole fractions (x) only. The need to take these into account in Calphad solution modelling was pointed out by Oates et al. [42] and, subsequently, its incorporation into the CEF was suggested by Sundman et al. [43]. Briefly, one can write

$$\Delta G = \Delta G(\text{CEF, config. dependent, } \textit{site fractions}) + \Delta G^{E}(\text{config. independent, } \textit{mole fractions})$$

or formally

$$G_m(\phi) = \sum_i \sum_j \sum_k y_i^1 y_j^2 y_k^3 \, {}^0G_{i:j:k} + RT \sum_s a_s \sum_i y_i^s \ln(y_i^s) + x_{Ni} x_V \sum_{n=0}^{(n)} L (x_{Ni} - x_V)^{(n)}$$

where ${}^{(n)}L$ are the adjustable excess Gibbs energy parameters. Although the configuration independent contributions can be related to the volume changes which occur on mixing, they may also have other origins and, from a Calphad viewpoint, are best handled as a parameterised Redlich–Kister equation in the mole fractions.

Such a modified CEF model has recently been incorporated into the ChemSage (model SUBE), Thermo-Calc and WinPhaD [44] software packages. It was found essential to use the above equation in order to obtain a satisfactory thermodynamic description of the Au–Cu system [45] since it is not possible to describe both the order/disorder temperatures and the enthalpies of mixing without the inclusion of the configuration independent term. The importance of this configurational independent term is also brought out in the present work in that it is was found impossible to obtain a satisfactory thermodynamic description of the Ni–V system without it. The stoichiometry chosen for the σ-phase was as before but with an important change. Mixing was allowed on all three sublattices, giving $(Ni,V)_{10}(Ni,V)_4(Ni,V)_{16}$. This increases the number of end-members to eight, but now the Gibbs energy curve is produced which stretches the whole composition range, and, therefore, lattice stability values are required for both V(σ) and Ni(σ). Optimisation was carried out using the WinPhad optimisation software.

The lattice stability of V(σ) was taken from Ref. [34] as before and that for Ni(σ) from Ref. [46]. The optimised parameters are given in Table 4, and the Gibbs energy curves calculated from these parameters are shown in Fig. 6. Although the interaction parameters are again numerically large, in this case, they do not refer to the interactions between the atoms on the individual sublattices, but to a configuration independent contribution to the total Gibbs energy of the phase. The Gibbs energy curve produced is much smoother than produced in the previous optimisation, and the consequences of this can be seen by the improved fit of the experimental phase diagram data to the calculated phase boundaries (Fig. 7). However, the σ-phase field boundaries begin to converge at lower temperatures despite the suggestion from the only set of experimental phase diagram information below the peritectoid decomposition temperature of the NiV_3 phase that this may not be the case. Some more work in this region of the diagram is required to improve the fit. The Ni-rich part of the curve exhibits kinks which are possibly a consequence of there being no experimental data in this part of the system for the σ-phase.

Table 4
Optimised parameters with the σ-phase described using the modified CEF with the $(Ni,V)_{10}(Ni,V)_4(Ni,V)_{16}$ stoichiometry. Parameters for solution phases are as in Table 2

Phase	Parameter	Value
Ni_2V	$\Delta_f G(Ni_{0.666}V_{0.333})$	− 15 158 + 2.64862**T*
Ni_3V	$\Delta_f G_{Ni:V}$	− 51 400.00 + 5.62961*T*
	$\Delta_f G_{Ni:Ni}$	4363.13 − 1.06473*T*
	$\Delta_f G_{V:V}$	32 000.00 + 6.8*T*
	$\Delta_f G_{V:Ni}$	87 763.00 + .10566*T*
	${}^0L_{Ni,V:*}$	−6520.17
	${}^1L_{*:V,Ni}$	414.67
sigma	$\Delta_f G_{(Ni:Ni:Ni)}$	313 800.00 + 125.52*T*
$(Ni,V)_{10}(Ni,V)_4(Ni,V)_{16}$	$\Delta_f G_{(Ni:V:Ni)}$	154 860.00 + 12.976*T*
	$\Delta_f G_{(Ni:Ni:V)}$	212 931.45 − 226.5477*T*
	$\Delta_f G_{(Ni:V:V)}$	− 76 580.55 + 380.3742*T*
	$\Delta_f G_{(Vi:Ni:Ni)}$	316 102.81 + 121.6633*T*
	$\Delta_f G_{(V:V:Ni)}$	188 140.85 − 113.2029*T*
	$\Delta_f G_{(V:Ni:V)}$	70 012.76 + 13.1178*T*
	$\Delta_f G_{(V:V:V)}$	200 010.00 + 23.1000*T*
	${}^0L$	2 015 282.34 + 684.0686
	${}^1L$	494 498.33 + 120.0000*T*
NiV_3	$\Delta G_f(Ni_{0.25}V_{0.75})$	−10 793.99 + 2.6202

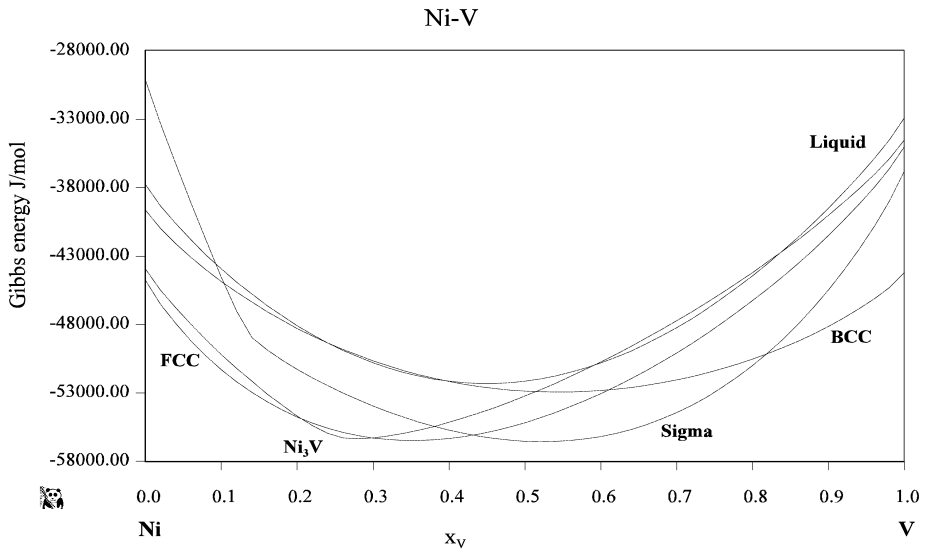

Fig. 6. Gibbs energy curves at 1000 K for phases in the Ni–V system, with the sigma phase calculated using the modified CEF, referred to HSER. The Gibbs energies of the stoichiometric phases have been omitted for clarity.

4. Discussion

From the above calculations, it can be seen that the σ-phase of the Ni–V system can be described with varying success by a number of different thermodynamic models. However, the choice of model is critical and is dependent on a number of criteria. It is desirable that the model should have some relationship with physical reality, and it is clear that a multiple sublattice model fulfills this criterion. But, as shown above, large values for the *L* parameters can result when using the CEF, but using the modified CEF can circumvent this as, in this model, the *L* parameters represent other quantities; even though in the present optimisation the improvement of the fit of the σ-phase/bcc boundary was at the expense of the fit to the fcc/σ-phase boundary. This reflects the difficulty in op-

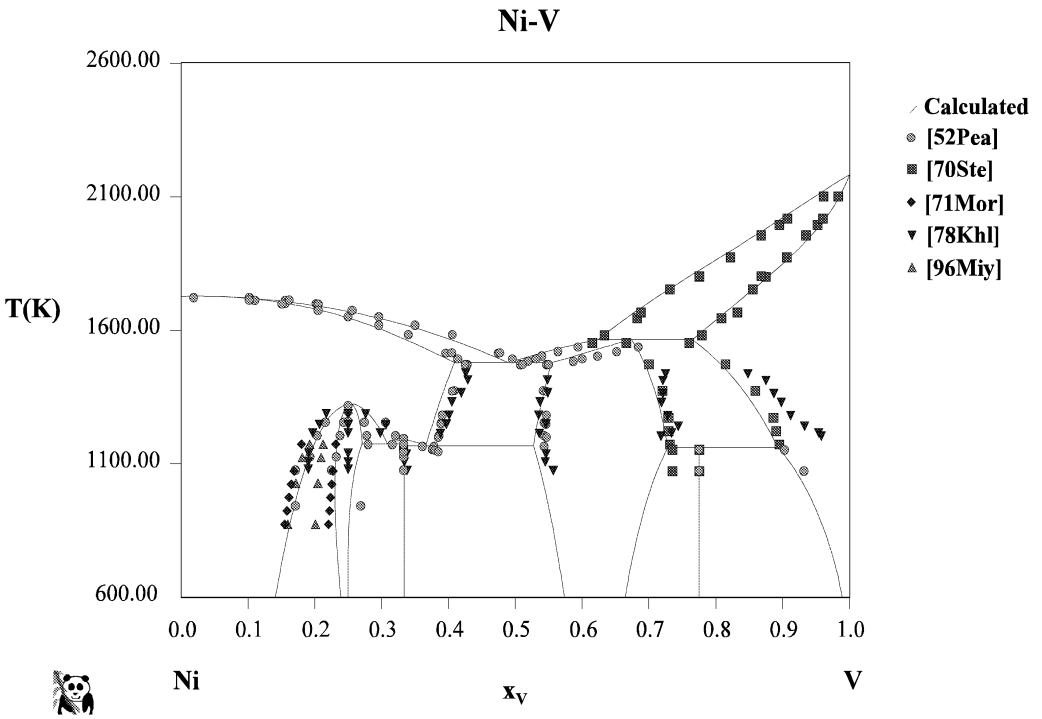

Fig. 7. The Ni–V phase diagram, calculated using the modified CEF model for the sigma phase.

timising using a model which has a relatively large number of end-member parameters. Work is required to improve this part of the diagram.

The modified CEF is a relatively new model, and using it can produce more problems. The power of computerised thermodynamic calculation is being able to perform complex equilibrium calculations using many components. This requires the same model to be used for phases that appear in more than one subsystem so as to be able to model extended solubilities in higher order systems. This would raise difficulties, for example, if the modified CEF dataset for the Ni–V system was used in conjunction with the dataset as recommended by the SGTE for the Fe–V system as the σ-phase in the latter system is described using the 18:4:8 stoichiometry. In such a case, it would be necessary to re-optimise using the modified CEF so that the mixing in the ternary could be modelled.

Undoubtedly, models to describe complex intermetallic phases are improving. But this is raising problems with regard to compatibility. In the long run, it would be expected that the *Calphad* approach would not only move closer to crystallography but also to the physics of the system as well.

Acknowledgements

Thanks are extended to Prof Alan Oates for fruitful discussions regarding the modified CEF and to Dr. Nathalie Dupin for help with its implementation into Thermo-Calc. Also to Dr. T.G. Chart for guidance in the early use of BINGSS, Dr. H.L. Lukas for provision of the software, The Materials Metrology Division, NPL, Teddington, UK, for use of the MTDATA software, Thermo-Calc AB, Stockholm, Sweden, for the provision of the Thermo-Calc software, and to Prof. Austin Chang and Fan Zhang at CompuTherm, Winsconsin, USA, for the use of WinPhad.

References

[1] E.O. Hall, S.H. Algie, Metall. Rev. 11 (1960) 61.
[2] I. Ansara, T.G. Chart, A. Fernadez-Guillermet, F.H. Hayes, U.R. Kattner, D.G. Pettifor, N. Saunders, K. Zeng, Calphad 21 (2) (1997) 171.
[3] J.F. Smith, O.N. Carlson, P.G. Nash, Bull. Alloy Phase Diagrams 3 (3) (1982) 342.
[4] J.F. Smith, O.N. Carlson, P.G. Nash, in: J.F. Smith (Ed.), Phase Diagrams of Binary Vanadium Alloys, American Society for Metals, Metals Park, OH, 1989.
[5] R. Luoma, Report TTK-V-B76, Helsinki University of Technology, Laboratory of Materials Processing and Powder Metallurgy, 1992.
[6] W.B. Pearson, W. Hume-Rothery, J. Inst. Met. 80 (1952) 641.
[7] P. Greenfield, P.A. Beck, Trans. AIME 200 (1954) 253.
[8] E.R. Stevens, O.N. Carlson, Metall. Trans. 1 (1970) 1267.
[9] V.S. Khlomov, V.N. Pimenov, Yu.E. Ugaste, K.P. Gurov, Fiz. Met. Metalloved. 46 (3) (1978) 668.
[10] T. Miyazaki, Private communication.
[11] T.B. Massalski, J.L. Murray, L.H. Bennet, H. Baker, Binary Alloy Phase Diagrams, American Society for Metals, Metals Park, OH, 1986.
[12] M. Daire, M. Gerspacher, J. Less-Common Met. 17 (1969) 334.
[13] H.A. Moreen, R. Taggart, D.H. Polonis, J. Mater. Sci. 6 (1971) 1425.
[14] K. Schaefers, J. Qin, M. Rösner-Kuhn, M.G. Frohberg, Can. Metall. Q. 35 (1) (1996) 47.
[15] A. Watson, F.H. Hayes, J. Alloys Comp. 220 (1995) 94.
[16] V.I. Alekseev, G.A. Levshin, Diffuzion. Protessy Metallakh. (1977) 112.
[17] V.I. Alekseev, G.A. Levshin, Izv. V. U. Z. Chernya Metall. 11 (1980) 19.
[18] B. Million, J. Vrestal, V.I. Patoka, V.I. Silantjev, V.N. Kolesnik, Czech. J. Phys. B 30 (1980) 541.
[19] V.I. Patoka, V.I. Silantjev, V.N. Kolesnik, J. Vrestal, B. Million, Czech. J. Phys. B 30 (1980) 465.
[20] I.I. Kornilov, N.P. Mateeva, Metall. I Gorn. Delo. Izv. Akad. Nauk SSSR 1 (1964) 143.
[21] Q. Guo, O.J. Kleppa, J. Phys. Chem. 99 (1995) 2854.
[22] J.H. Perpezko, in Ref. [4].
[23] A.T. Dinsdale, Calphad 15 (1991) 317.
[24] O. Redlich, A.T. Kister, Ind. Eng. Chem. 2 (1948) 345.
[25] C. Wagner, Thermodynamics of Alloys, Addison-Wesley, Cambridge, MA, 1952.
[26] H.L. Lukas, S. Fries, U. Kattner, J. Weiss, BINGSS, BINKFT, TERGSS and TERFKT Reference Manual, Version 95-1, January 19, 1995.
[27] H.L. Lukas, E.Th. Henig, B. Zimmermann, Calphad 1 (3) (1977) 225.
[28] I. Ansara, Int. Met. Rev. 1 (1979) 20.
[29] J.S. Kasper, R.M. Waterstrat, Acta Crystallogr. 9 (1956) 289.
[30] J.-O. Andersson, B. Sundman, Calphad 11 (1987) 83.
[31] W. Huang, Trita-Mac-0432, KTH, Stockholm, Sweden, 1989.
[32] R.H. Davies, A.T. Dinsdale, T.G. Chart, T.I. Barry, M.H. Rand, High Temp. Sci. 26 (1990) 251.
[33] C. Servant, I. Ansara, J. Chim. Phys. 94 (5) (1997) 869.
[34] F.H. Hayes, R. Kubitz, Project Meeting, Calphad VII, Stuttgart, 1978, p. 190.
[35] B. Sundman, B. Jansson, J.-O. Andersson, Calphad 9 (1985) 153.
[36] J.D. Eshelby, in: F. Seitz, D. Turnbull (Eds.), Solid State Physics, Vol. 3, Academic Press, New York, 1956, p. 79.
[37] W.A. Oates, A.M. Stoneham, J. Phys. F: Met. Phys. 13 (1983) 2427.
[38] R. Bass, H.R. Schober, W.A. Oates, A.M. Stoneham, J. Phys. F: Met. Phys. 14 (1984) 2869.
[39] L.G. Ferreira, A.A. Mbaye, A. Zunger, Phys. Rev. B 35 (1987) 6475.
[40] J.-O. Andersson, A. Fernandez-Guillermet, M. Hillert, B. Jansson, B. Sundman, Acta Metall. 34 (1986) 437.
[41] M. Hillert, Phase Equilibria, Phase Diagrams and Phase Transformations — Their Thermodynamic Basis, Cambridge University Press, 1998.
[42] W.A. Oates, H. Wenzl, T. Mohri, Calphad 20 (1996) 1.
[43] B. Sundman, S.G. Fries, W.A. Oates, Calphad 22 (3) (1998) 355.
[44] WinPhaD 2.0 — A new tool that simplifies the calculation of phase diagrams and thermodynamic properties in binary systems.
[45] B. Sundman, S.G. Fries, W.A. Oates, Calphad 22 (3) (1998) 335.
[46] L. Kaufman, L. Bernstein, Computer Calculations of Phase Diagrams, Refractory Series Monograph, Vol. 4, Academic Press, New York, 1970.